GLOBAL BIOGEOCHEMICAL CYCLES, VOL. 11, NO. 3, PAGES 393–400, SEPTEMBER 1997

# Timescales in atmospheric chemistry: $CH_3Br$, the ocean, and ozone depletion potentials

Michael J. Prather

Department of Earth System Science, University of California at Irvine

**Abstract.** Methyl bromide ($CH_3Br$) supplies about half of the chemically active bromine ($Br_y$) in the stratosphere. Efforts to control $Br_y$-catalyzed ozone depletion by phasing out, for example, agricultural use of $CH_3Br$ may be thwarted by a lack of understanding of how the varied biogeochemical processes interact as a coupled system: in addition to the chemical industry, large natural sources come from the ocean; and losses occur in the atmosphere, ocean, and soils. A simplified one-dimensional stratosphere-troposphere-ocean model for {$CH_3Br$, $Br_y$} that fits current understanding of sources and sinks is analyzed in terms of natural modes. Surface and ocean sources have effectively different steady state lifetimes (1.0 and 0.5 years, respectively), but the natural-mode decay times of the system (1.8 years for $CH_3Br$ and 4.5 years for stratospheric $Br_y$) do not depend on the location of sources. The cumulative ozone depletion resulting from a single atmospheric release of $CH_3Br$ integrates over the consequent slow rise and fall of $Br_y$ in the lower stratosphere. Thus, in spite of the 1-year lifetime of $CH_3Br$, only half of the anticipated ozone recovery occurs in the first 7 years.

## 1. Introduction

Protection of the stratospheric ozone layer, our shield against damaging solar ultraviolet radiation, has been largely achieved through international protocol [*Montreal*, 1987]. The idea that human activities could severely deplete the ozone on a global scale was first proposed [*Crutzen*, 1970; *Johnston*, 1971; *Molina and Rowland*, 1974] and then established in the last 3 decades through the individual research of many scientists and the international scientific assessments [*World Meteorological Organization (WMO)*, 1986, 1992, 1995]. It was recognized by the award of the 1995 Nobel Prize in Chemistry to Crutzen, Molina, and Rowland. Many trace gases measured in the stratosphere are changing as a result of human activity and are identified with potential ozone depletion: odd-nitrogen [*Johnston*, 1971; *McElroy et al.*, 1977]; chlorine [*Molina and Rowland*, 1974; *Stolarski and Cicerone*, 1974]; methane [*Ehhalt*, 1974]; and bromine [*Wofsy et al.*, 1975]. Of all, bromine is the most potent on a molecule-per-molecule basis.

The primary source gases identified with transporting bromine into the stratosphere have been well measured [*Schauffler et al.*, 1993]. Their decay in the stratosphere is consistent with the release of chemically active bromine ($Br_y$), in particular BrO, the primary bromine radical in the catalytic destruction of ozone [*Brune et al.*, 1989; *Carroll et al.*, 1989; *Toohey et al.*, 1990]. Currently identified sources of stratospheric bromine are methyl bromide ($CH_3Br$, 10 parts per trillion (ppt)), halon-1211 ($CF_2ClBr$, 3.4 ppt), halon-1301 ($CF_3Br$, 2.3 ppt), and halon-2402 ($CF_2BrCF_2Br$, 0.7 ppt) [*WMO*, 1995; *Schauffler et al.*, 1993; *Montzka et al.*, 1996]. Production of halons is already phased out under the amended Montreal Protocol, so attention focuses on $CH_3Br$ as a potential quick fix [*WMO*, 1995] to ameliorate the peak ozone depletion expected over the next decade [*Jackman et al.*, 1996; *Prather et al.*, 1996]. This paper examines our ability to control the abundance of methyl bromide and the consequent ozone depletion.

Atmospheric $CH_3Br$ comes in part from agricultural and other industrial uses of this compound [*McCulloch*, 1992; *Duafala*, 1995], but its abundance appears to be buffered by a large oceanic biological source and an oceanic chemical sink [see *Butler*, 1994; *Elliott and Rowland*, 1993; *Lobert et al.*, 1995; *Yvon and Butler*, 1996; *Anbar et al.*, 1996]. Current assessments have assumed a simple e-folding model for the impact of anthropogenic $CH_3Br$ emissions, using a global-mean atmospheric lifetime of 1.3 years that includes atmospheric and oceanic losses, but not the recently discovered soil sink [*Shorter et al.*, 1995]. It is shown here that the simple exponential decay, adequate for long-lived gases like halon-1301, does not describe the atmospheric response of $CH_3Br$, nor the rate of ozone recovery.

This paper presents a one-dimensional (1-D) time-dependent stratosphere-troposphere-ocean model for $CH_3Br$ and $Br_y$ in section 2 and uses natural modes [*Prather*, 1994, 1996] to study the temporal behavior of this system for changes in $CH_3Br$ emissions. The spatial patterns and $e$-fold timescales of the modes are derived in section 3. Several constants for geochemical systems can be defined with units of time: global-mean lifetime, which is based on budgets (total content divided by the sum of all loss rates); mean lifetime against loss



Paper number 97GB01055.
0886-6236/97/97GB-01055$12.00

in one reservoir (total-content / reservoir-loss); turnover time of an individual reservoir (inverse of loss frequency *[Bolin and Rodhe,* 1973]); and the inverse eigenvalues of the linearized differential equations [*Prather,* 1994]. It is these latter constants which are the true timescales describing how the atmosphere responds to anthropogenic $CH_3Br$ emissions. Such response is not affected by the magnitude of the oceanic source. The removal of stratospheric $Br_y$ (and hence the recovery of ozone) proceeds at a much slower rate, independent of the $CH_3Br$ timescales. Section 4 compares the ozone depletion potentials (ODPs) derived from assessments with those from the true time-dependent evolution of $CH_3Br$ and $Br_y$. Section 5 compares natural modes and their timescales with different steady state solutions and considers what other chemical systems may yield unexpected results.

## 2. A 1-D Chemical-Diffusion Model

The {$CH_3Br$, $Br_y$}-system can be represented by a one-dimensional diffusive atmosphere [e.g., *Logan et al.,* 1978] with additional exchange between an ocean layer and the lowest atmospheric layer. $CH_3Br$ is destroyed primarily by OH reaction in the troposphere, by photolysis in the stratosphere, by reaction in soils, and by nucleophilic displacement and hydrolysis in the ocean. The bromine species formed after atmospheric destruction of $CH_3Br$ (i.e., Br, BrO, HBr, HOBr, $BrONO_2$) are designated collectively as $Br_y$. (Ozone depletion is assumed to be proportional to stratospheric $Br_y$, and this paper considers only the $Br_y$ from $CH_3Br$.) Production of $Br_y$ matches loss of $CH_3Br$, and $Br_y$ is conserved in the stratosphere but washed out in the troposphere. The continuity equations (1) for the densities of $CH_3Br$ and $Br_y$ can be written in terms of the emissions P and loss frequencies L for each layer, and the divergence of the diffusive flux $\nabla\phi$. This model, defined in Table 1, is taken as linear in that $CH_3Br$ does not perturb OH concentrations or oceanic hydrolysis rates. (The possible coupling of $Br_y$ with ozone depletion and enhanced UV is not considered.)

$$d[CH_3Br]/dt = -\nabla\phi_{CH3Br} + P_1 - L_1\,[CH_3Br] \qquad (1)$$

$$d[Br_y]/dt = -\nabla\phi_{Bry} + L_1\,[CH_3Br] - L_2\,[Br_y]$$

Consider the atmosphere alone (designated case B1, no ocean). A steady state distribution forced from surface emissions of $CH_3Br$ is calculated by integrating the coupled diffusion equation (1) for several decades. The resulting profiles of $CH_3Br$ and $Br_y$ are shown by the thick lines in Figures 1a and 1b, respectively. This pattern is typical of the halocarbon source gases: well mixed tropospheric abundance, falling off slowly in the lower stratosphere and more rapidly in the upper stratosphere, coinciding with the release of $Br_y$ in the stratosphere such that the sum of mixing ratios, $CH_3Br$ + $Br_y$, is constant through the stratosphere. The steady state lifetime of $CH_3Br$, 1.75 years, is computed as the total abundance (157 kt for 10 ppt at the surface) divided by the mean annual loss (90 kt/yr), which at steady state balances emissions.

What happens if emissions cease? Consider a hypothetical case in which all sources responsible for 10 ppt of $CH_3Br$ are cut. Figure 1 follows the evolution of both profiles (thin lines, labeled with the year after cutoff). The $CH_3Br$ profile decays with a timescale of about 2 years and changes shape. The $Br_y$ profile maintains the same basic shape, does not change much over the first 2 years, and then decays much more slowly than does $CH_3Br$. The $CH_3Br$ decay is summarized in Figure 2. It begins with a 1.75-year *e*-folding but asymptotically approaches a 2.1-year *e*-folding. The decay time for stratospheric $Br_y$, however, is about 4.5 years. Neither of these decay times is reflected in the steady state lifetime. The decay patterns and their *e*-folding times are identical to the natural modes and their timescales [*Prather,* 1996] as derived in section 3.

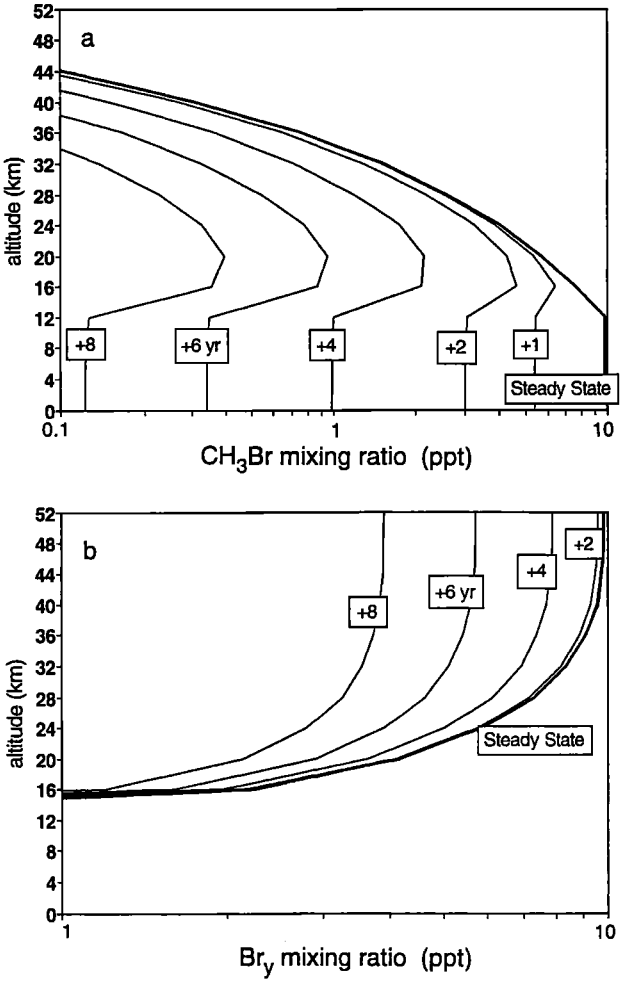


**Figure 1.** (a) Profile of $CH_3Br$ mixing ratio (parts per trillion) versus altitude (kilometers) at steady state driven by surface emissions (thick line). Also shown are the profiles following cutoff of $CH_3Br$ emissions (thin lines labeled by the years since cutoff). (b) Profile of $Br_y$ mixing ratio versus altitude at steady state (thick line), also showing decay following cutoff (thin lines). Model is case B1 (atmosphere alone) described in Table 1.

Global lifetimes or individual reservoir turnover times are often mistakenly thought to be true timescales of the system's response to a perturbation. Figure 3 presents block diagrams of the $CH_3Br$ contents (kilotons) and fluxes (kilotons/yr) for three cases: B1, no ocean (Figure 1); B2, an oceanic sink but no source; and B3, an oceanic source to match the observed average 85% saturation. All numbers refer to a steady state with 10 ppt at the surface; see also Table 1. The global

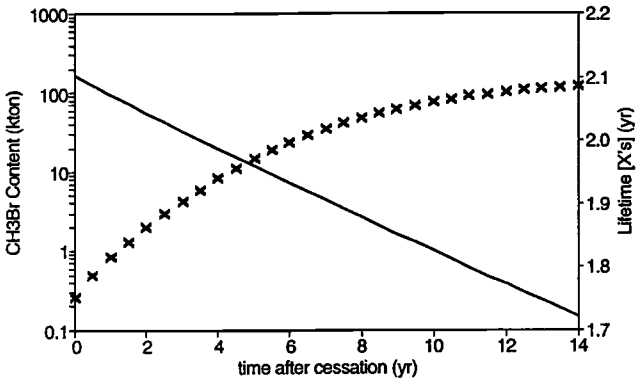


**Figure 2.** Decay of $CH_3Br$ atmospheric content (kilotons) from a steady state following cutoff of emissions (solid line, left axis) and the derived instantaneous lifetime (years) (crosses, right axis). The decay begins with the steady state lifetime, 1.75 years, and approaches 2.10 years, the timescale of the primary natural mode of $CH_3Br$ (case B1, Figure 1a).

atmospheric lifetime in B1, 1.75 years, is in steady state (i.e., emissions equal total losses) but not obviously related to the 2.1-year long-term decay time found above. In B2 two definitions of lifetime are possible, 1.01 and 1.03 years, depending on whether the oceanic content is included in the content. As shown below, 1.03 years is the correct interpretation, but neither of these accurately describe the temporal response of the atmosphere plus ocean system. The definition of lifetime is even more ambiguous in case B3 where inclusion of the an oceanic source allows one to calculate an atmospheric lifetime of 1.46 years (because less surface emissions go into the ocean) or a global lifetime of 0.76 years for the combined source. (This latter value applies if we perturb both sources proportionally.) Cases B2 and B3 demonstrate the sensitivity of lifetimes to the location of sources, since both cases have the same chemical-physical system and hence identical modes and timescales.

While the time-dependent response of this system to various perturbations can be accurately calculated using the continuity equations (1), simple use of global-mean lifetimes or reservoir turnover times is inaccurate. Analysis of the system in terms of its natural modes and their timescales gives identical results to the numerical solution but provides insight into the patterns that evolve and allows for accurate prediction under different forcing, as shown next.

## 3. Natural Modes of the $\{CH_3Br, Br_y\}$ System

In atmospheric chemistry the continuity equation (2) for the concentration of each species at a given spatial location $x_i$ can be expressed in terms of its local net chemical production $p_i$ and its transport tendency $\nabla\phi_i$ (i.e., the flux divergence). We solve equation (2) for the mixing ratio, $f_i = x_i/N$, where N is the concentration of background air. The index i covers m species at n spatial locations. The nm×nm Jacobian matrix **J** (equation (3)) is defined as the partial derivative of each equation with respect to each independent variable. In a 1-D diffusion model the flux is down-gradient, $\phi_i = -K\, dx_i/dz$ (vertical dimension z, diffusion coefficient K), and its divergence in equation (3) can be expressed as a finite-difference equation involving nearest neighbors. The Jacobian matrix **J** is then block tridiagonal (equation (4)). The 2×2 diagonal blocks **P+T** include the real asymmetric chemical Jacobian plus the transport coefficients. The upper and lower diagonal blocks **T** are diagonal matrices with only transport coefficients (e.g., $KN/\Delta z^2$). The boundary conditions **B** are matrices that couple species in the lowermost two layers and also, separately, the uppermost two layers.

$$N\, df_i/dt = dx_i/dt = p_i - \nabla\phi_i \qquad (2)$$

$$\mathbf{J}_{ik} \equiv \partial(df_i/dt)/\partial f_k = \partial(p_i/N)/\partial f_k - \partial(\nabla\phi_i/N)/\partial f_k \qquad (3)$$

$$\mathbf{J} = \begin{bmatrix} \mathbf{B} & \mathbf{B'} & 0 & 0 & \cdots & 0 & 0 & 0 & 0 \\ \mathbf{T'} & \mathbf{P+T} & \mathbf{T''} & 0 & \cdots & 0 & 0 & 0 & 0 \\ 0 & \mathbf{T'} & \mathbf{P+T} & \mathbf{T''} & \cdots & 0 & 0 & 0 & 0 \\ & & & & \cdots & & & & \\ 0 & 0 & 0 & 0 & \cdots & \mathbf{T'} & \mathbf{P+T} & \mathbf{T''} & 0 \\ 0 & 0 & 0 & 0 & \cdots & 0 & \mathbf{T'} & \mathbf{P+T} & \mathbf{T''} \\ 0 & 0 & 0 & 0 & \cdots & 0 & 0 & \mathbf{B'} & \mathbf{B} \end{bmatrix} \qquad (4)$$

The nm eigenvectors of **J**, $A^k$, span the space of chemical species. The corresponding eigenvalues $-c_k$ describe the *e*-folding frequency (per second) of that eigenvector. Any species distribution S (i.e., vertical profiles of both $CH_3Br$ and $Br_y$) can be expressed as a sum of these eigenvectors (natural modes) (equation (5)). The set $A^k$ is linearly independent but unfortunately not orthogonal; hence, the complete set is needed to create the **A** matrix and solve for the coefficients of each mode, $s_k = (\mathbf{A}^{-1}\, S)_k$. (If the $A^k$ were orthogonal, then each coefficient $s_k$ can be calculated from each $A^k$ alone.) The decay of that distribution S is exactly the *e*-folding of the individual modes at their characteristic timescales of $1/c_k$ (equation (6)).

$$S(0) = \sum_{k=1:nm} s_k\, A^k \qquad (5)$$

$$S(t) = \sum_{k=1:nm} s_k\, A^k \exp[-c_k t]. \qquad (6)$$

For the $\{CH_3Br, Br_y\}$ system without an ocean layer the **J** matrix (equation (4)) is 28×28 (n=14, m=2), and there are 28

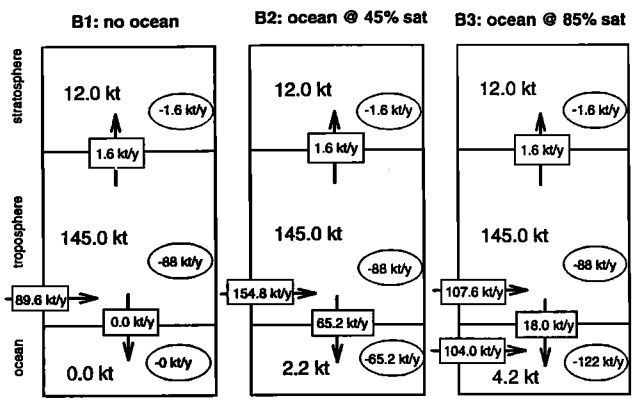


**Figure 3.** Block diagrams of $CH_3Br$ content (kilotons) and fluxes (kilotons per year) for the stratosphere-troposphere-ocean reservoirs at a steady state (10 ppt in the lower atmosphere). Soil sink is included in tropospheric loss. The three cases are no ocean (B1, see text), ocean sink but no source (B2), and both surface and oceanic sources matched to 85% saturation in the ocean layer (B3).

**Table 1.** Analysis of Global Lifetimes at Steady State

| | B1 | B3/S[a] | B3/O |
|---|---|---|---|
| $CH_3Br$ at 0 km, ppt | 10.0 | 7.0 | 3.0 |
| $CH_3Br$ in ocean (vapor pressure), ppt | --- | 4.5 | 4.0 |
| $Br_y$ at 20 km | 4.17 | 2.90 | 1.27 |
| $CH_3Br$ content | | | |
| Stratosphere, kt | 12.0 | 8.3 | 3.7 |
| Troposphere, kt | 145.0 | 100.8 | 44.2 |
| Ocean, kt | --- | 1.5 | 2.7 |
| $CH_3Br$ losses | | | |
| Stratosphere, kt/yr | 1.6 | 1.1 | 0.5 |
| Troposphere, kt/yr | 88.0 | 61.2 | 26.8 |
| Ocean, kt/yr | --- | 45.3 | 76.7 |
| $CH_3Br$ emissions | | | |
| Surface, kt/yr | 89.6 | 107.6 | --- |
| Oceanic, kt/yr | --- | --- | 104.0 |
| Global lifetime against loss in each reservoir | | | |
| Stratosphere, years | 98. | 100. | 101. |
| Troposphere and soils, years | 1.78 | 1.81 | 1.89 |
| Ocean, years | --- | 2.44 | 0.66 |
| Global lifetime (inverse sum of above), years | 1.75 | 1.03 | 0.49 |

[a]B3 (Figure 3) is split into surface (/S) and oceanic (/O) sources.

modes. Since the $CH_3Br$ solution is independent of $Br_y$, one expects that only 14 modes describe the $CH_3Br$ distribution, and indeed only 14 of the 28 modes have nonzero elements for $CH_3Br$. These modes as shown in Figure 4 (dimensionless, relative perturbations in the mixing ratio) can be combined uniquely to describe any vertical profile of $CH_3Br$. Short-lived modes are clearly associated with nearest-neighbor transport. The timescales of the stratospheric modes become slower in the lower stratosphere near the diffusion minimum. All of the modes change sign except the longest, primary mode which must have one sign since it is the final pattern that decays. In spite of these negative concentrations in each mode, the sum of modes corresponding to any positive distribution (equation (5)) remains positive throughout its decay (equation (6)). The primary 2.10-year mode represents the decay pattern of a gas that is photolyzed rapidly in the upper stratosphere and also removed quickly in the troposphere (see decay of $CH_3Br$ profile in Figure 1a). Increasing the spatial resolution (i.e., degrees of freedom) leads to a corresponding increase in the number of short-lived modes corresponding to nearest-neighbor transport but does not substantially alter the primary mode.

For the {$CH_3Br$, $Br_y$} system with an ocean layer, the **J** matrix (equation (4)) is 30×30 (n=15, m=2), and there are 30 modes of which 15 describe $CH_3Br$ patterns as shown in Figure 5. Comparing Figures 4 and 5, one can identify the additional mode (0.021 years) that is most closely associated with the ocean layer (labeled -4 km). All other modes look similar to the atmosphere-alone case. The addition of a degree of free-dom (the ocean layer) shifts many but not all of the modes and creates a new one that is not just the ocean chemical turnover time (~0.03 years), but a coupling of that with the atmospheric reservoir. Timescales for the nearest-neighbor transport are unchanged. With this additional sink those modes representing more global patterns, such as the primary mode, have a shorter timescale, 1.83 versus 2.10 years. The modes couple all reservoirs and chemical losses; and thus, the patterns cannot always be identified uniquely with the additional component.

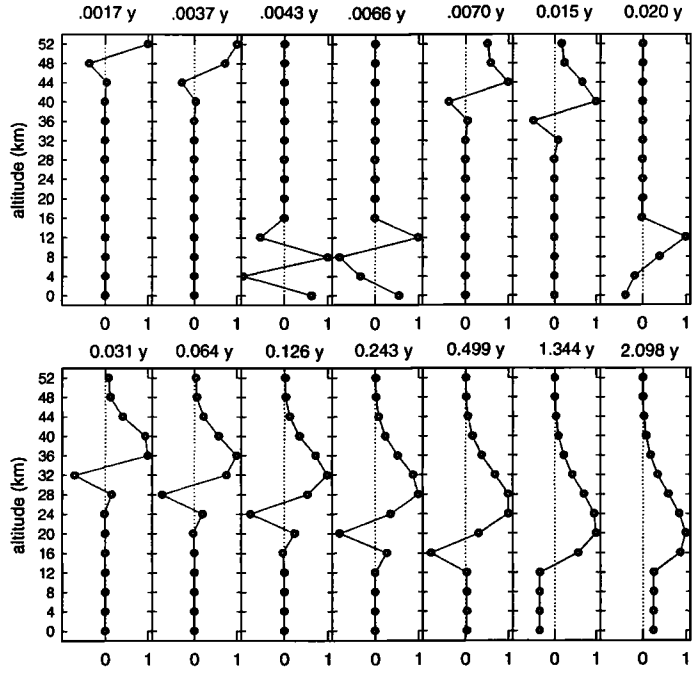


**Figure 4.** The complete set of 14 natural modes for $CH_3Br$ in the case with no ocean (case B1). Each vertical pattern in the mixing ratio of $CH_3Br$ from 0 to 52 km is dimensionless and labeled with its corresponding timescale.

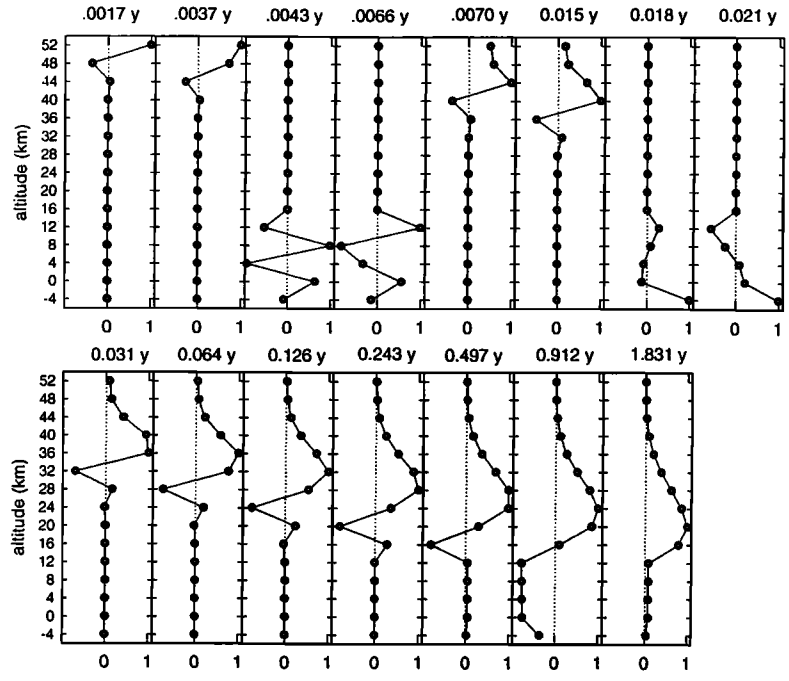


**Figure 5.** The complete set of 15 natural modes for $CH_3Br$ in the case with an ocean sink (cases B2 and B3). Each vertical pattern in the mixing ratio of $CH_3Br$ from -4 km (ocean layer) to 52 km is dimensionless and labeled with its corresponding timescale.

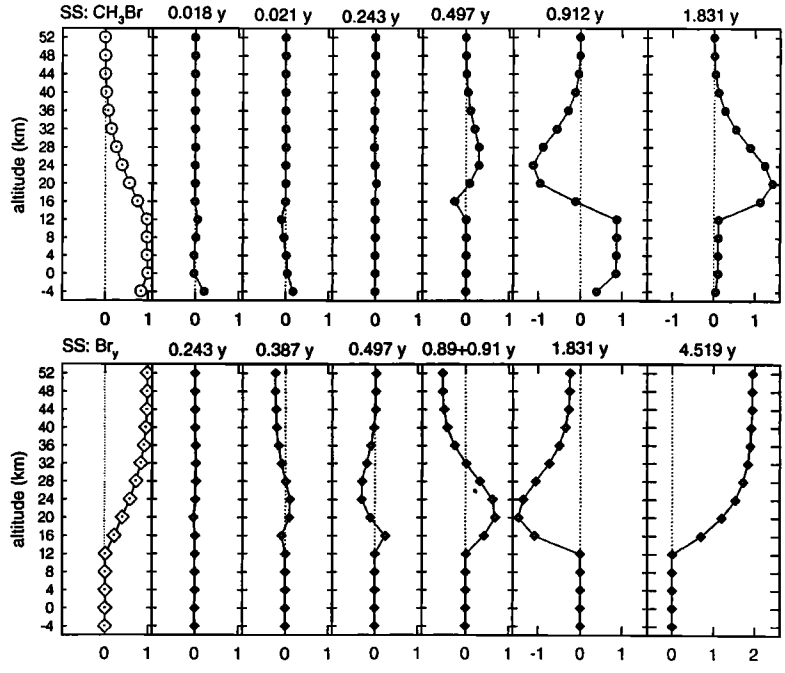


**Figure 6.** Decomposition of a steady state distribution (SS) of $CH_3Br$ (parts per trillion) and $Br_y$ (parts per trillion) into natural modes. The steady state is forced by both surface and oceanic emissions to achieve 1 ppt $CH_3Br$ in the lower atmosphere and 85% saturation in the ocean (case B3). Each scaled mode (parts per trillion) is multiplied by the coefficient derived from the SS distribution and is labeled with its *e*-folding timescale. Two of the $Br_y$ modes (0.892 and 0.912 years) are nearly degenerate and have been combined.

The steady state distribution (SS) of $CH_3Br$ and $Br_y$ resulting from a combination of surface and oceanic emissions (B3) is shown in Figure 6. The source was scaled to give 1 ppt of $CH_3Br$ in the lower atmosphere and 85% saturation in the ocean layer. These profiles are shown with the open symbols in the left-hand panels. The SS:$CH_3Br$ profile is comprised of all the 15 modes in Figure 5, but only those with significant coefficients $s_k$ are shown as scaled modes (in units of parts per trillion) in Figure 6. Except for the stratospheric-readjustment mode (0.497 years), the SS profile is predominantly a combination of the two longer-lived modes (0.912 and 1.831 years). The SS:$Br_y$ profile is comprised of the full 30 modes (not shown), and those with the largest coefficients $s_k$ are shown here. Some of these scaled modes (0.387, 0.89, and 4.519 years) are unique to $Br_y$ and have no $CH_3Br$ elements. The 0.89-year and 0.91-year modes have been combined since they are nearly degenerate with large and cancelling coefficients. The primary 4.519-year mode represents the removal of a conserved trace gas from the stratosphere (compare with decay profile in Figure 1b). Note that this long-lived mode has amplitude 2 ppt in the upper stratosphere, being balanced by negative mixing ratios from the other modes, and explains why the profile of $Br_y$ in Figure 1b hardly changes in the first 2 years.

Once the **A** matrix of modes has been calculated as in Figure 5, the exact, time-dependent response to any perturbation may be readily derived. Consider a single, pulsed emission equivalent to a surface source (all $CH_3Br$ in the 0-km atmospheric layer, labeled PE:$CH_3Br$ in the left panel of Figure 7). This profile has been scaled to have the same total content as SS:$CH_3Br$ in Figure 6, and the scaled modes (units of parts per trillion) comprising PE:$CH_3Br$ are shown with their timescales. Two short-lived modes (0.004 and 0.007 years) represent rapid tropospheric mixing; others involve exchange with the ocean layer; and the three longest-lived modes are similar to those for SS:$CH_3Br$ but with different amplitudes.

The $CH_3Br$ modes shift smoothly with changes in the chemical model. For example, if *Yvon and Butler*'s [1996] updated mean oceanic loss of 15%/d for $CH_3Br$ is used, the timescales of the two major modes shift from 1.83 to 1.81 years and from 0.91 to 0.82 years. The steady state lifetime for surface emissions drops from 1.03 to 0.91 years. Assuming 20% undersaturation of $CH_3Br$ in the ocean layer, the implied surface emissions of 113.5 kt/yr maintain an atmospheric abundance of 6.5 ppt at 0 km (versus 7.1 ppt in case B3), and oceanic sources maintain a background level of 3.5 ppt.

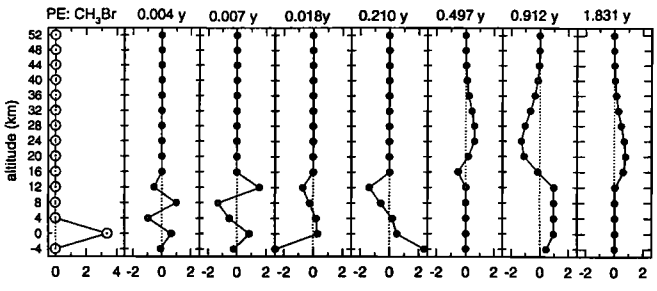


**Figure 7.** Decomposition of a single pulsed emission (PE) of $CH_3Br$ at the surface into scaled modes of $CH_3Br$ (parts per trillion). The total content of the PE case (3.4 ppt in 0-km layer) is the same as that of the SS profile of Figure 6.

## 4. ODPs and the Transient Response

The ozone depletion potential (ODP) for a halocarbon is meant to measure the cumulative environmental impact (i.e., $O_3$ depletion) from a single release of a gas ratioed to that from an equal release of $CFCl_3$. Instead of being computed as the true transient response following release of the gas, this cumulative impact is assumed to be the product of (1) the global-mean steady state lifetime and (2) the steady state concentration of active chlorine/bromine in the stratosphere corresponding to the amount of source gas emitted [e.g., *WMO*, 1995]. This approximation is rigorously correct as proven by *Prather* [1996], although the timescale is misleading as seen in Figure 1, and further, the steady state lifetime must be calculated using the comparable emission pattern.

The true transient response of $CH_3Br$ or $Br_y$ can be written exactly for any altitude in terms of the modes (equation (6)) for decay from SS (Figure 6) or for evolution of a pulsed emission (PE, Figure 7). For most assessments or policy options the focus is on the perturbation (positive or negative) caused by a change in emissions (positive or negative) for a given year-long PE. Any combination of actions, including a long-term change in emissions, can be expressed as a sum of PE cases.

The PE transients give the history of a single pulse, which is meant to be integrated by the ODP. $CH_3Br$ at 0 km (equation (7)) begins at 3.38 ppt and evolves as a mix of rapidly and more slowly decaying terms that integrate (product of coefficients and timescales, $1/c_k$) to 1.03 ppt yr. The coefficients of each exponential in equation (7) are the 0-km values in Figure 7. The content is scaled to the steady state profile of 1 ppt. A theorem equates the integral to the SS lifetime multiplied by the SS mixing ratio [*Prather*, 1996]. The correct lifetime is 1.03 years. Indeed, the corresponding equation for the SS $CH_3Br$ at 0 km (from Figure 6) can be easily calculated by integrating over an infinite prehistory of pulsed emissions, that is multiplying the coefficient in equation (7) by the $e$-folding time and dividing by 1.03. Stratospheric $Br_y$ (20 km) begins at 0.00 ppt with a large number of cancelling terms. The rapid decay of some negative coefficients leads to a rising concentration which eventually decays with the 4.52-year mode (equation (8)). The integral of the $Br_y$ transient is 0.43 ppt yr, which equals 1.03 years multiplied by 0.417 ppt (the SS $Br_y$ at 20 km for 1 ppt $CH_3Br$ in the lower atmosphere). The reason that this same theorem appears to work for $Br_y$ using the $CH_3Br$ lifetime is due to the complementary nature of $CH_3Br$ and $Br_y$ in the stratosphere.

$$\begin{aligned} CH_3Br^{PE}(t, 0\ km) &= 0.060e^{-t/1.831} + 0.964e^{-t/0.912} \\ &+ 0.029e^{-t/0.497} + 0.522e^{-t/0.021} + 0.300e^{-t/0.018} \\ &+ 0.858e^{-t/0.007} + 0.644e^{-t/0.004}\ ppt \end{aligned} \quad (7)$$

$$\begin{aligned} Br_y^{PE}(t, 20\ km) &= 0.273e^{-t/4.519} - 0.818e^{-t/1.831} \\ &+ 10.754e^{-t/0.912} - 10.187e^{-t/0.892} - 0.217e^{-t/0.497} \\ &+ 0.247e^{-t/0.387} - 0.096e^{-t/0.243} + 0.045e^{-t/0.207}\ ppt \end{aligned} \quad (8)$$

Figure 8 shows the transient response of $Br_y$ at 20 km to a single release of $CH_3Br$ equal in mass to the steady state distribution with a surface mixing ratio of 1 ppt (equation (8)). More than 99% of the tropospheric $CH_3Br$ is lost in the 5 years following emission. Stratospheric $Br_y$ levels just begin to peak then. About 25% of the $O_3$ depletion occurs more than 10 years after the emission of $CH_3Br$. The corollary is that a cut in $CH_3Br$ emissions yields recovery of $O_3$ only on a timescale of 5 to 15 years. The typical approach in calculating the halogen loading of the stratosphere [*Prather and Watson,* 1990] or the time-dependent ODP [*Solomon and Albritton,* 1992] is to shift the steady state pattern by 2 to 3 years to account for the delay in the source gas reaching the stratosphere (as calculated by *WMO* [1995, Figures 13-5 and 6]). However, for short-lived gases such as $CH_3Br$ and for short time horizons this shift does not accurately account for the slow buildup and decay of the ozone-depleting products in the stratosphere and can greatly overestimate the time-dependent ODP for horizons less than 10 years.

## 5. Timescales and Steady State

Natural modes are a mathematically rigorous, fundamental property of the chemical-transport system (i.e., current atmosphere) and do not depend on the manner of perturbation. Exponential decay of each natural mode with its own timescale is an exact solution in the limit of linear behavior. A unique mixture of modes is excited by any perturbation. For tightly coupled nonlinear chemical systems such as {$CH_4$, CO, OH} the use of natural modes clearly defines the timescales

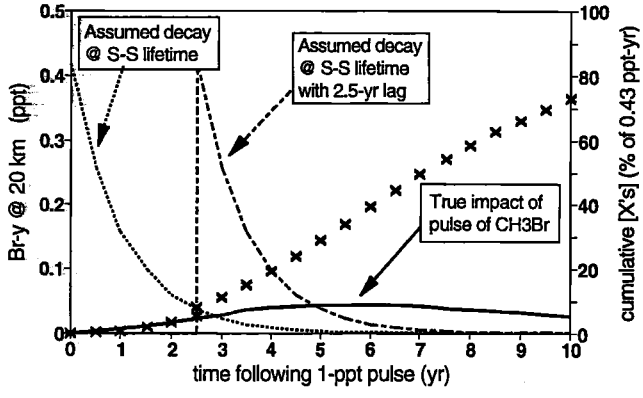


**Figure 8.** History of $Br_y$ at 20 km (i.e., ozone depletion) due to a single pulsed emission of $CH_3Br$ from the surface (Figure 7). The pulse has the same content as a steady state solution with 1 ppt $CH_3Br$ at 0 km (Figure 6). The true time-dependent growth and decay (solid line) can be calculated from the natural modes or by integrating the time-dependent equation (1). The often assumed history (dotted line) shows the steady state con-centration of $Br_y$ at 20 km (0.417 ppt) decaying with the global-mean lifetime (1.03 years). Time-dependent ozone depletion potentials (ODPs) often shift this curve by 2.5 years to account for the lag time for $CH_3Br$ to reach the stratosphere (dotted line). The area under all three curves is identical (0.43 ppt yr) but the true response (solid line) is much slower; for example, more than 1/4 of the impact occurs beyond 10 years.

and shows how perturbations to one species couple across all. For the simple atmospheric chemistry of the {$CH_3Br$, $Br_y$} system here the timescales of transport and chemistry are combined into the timescales of the long-lived, global modes. These modes, in various combinations, describe most transient and steady state responses to varied patterns of emissions. Because of this simple behavior, identification of the natural modes in current multi-dimensional atmospheric chemistry-transport models, while extremely difficult, would be valuable in diagnosis and also for prediction.

The steady state lifetime and distribution can be defined in terms of the natural modes. $CH_3Br$ provides a stunning example of how this steady state depends on the manner of forcing. For the atmosphere alone (B1), using Table 1 and Figure 3, the lifetimes of $CH_3Br$ against stratospheric loss (98 years) and tropospheric loss (1.78 years) combine to give the total steady state lifetime for a distribution forced by surface emissions (1.75 years = inverse of the sum of inverses). For the more realistic case with both surface and oceanic emissions (B3) the two different sources can be separated using case B2. In Table 1 the diagnostics split B3 into that component due to surface emissions (7 ppt at 0 km) and that due to oceanic emissions (3 ppt at 0 km). (This result is based on the assumed saturation, exchange rates, etc. in the 1-D model and is not intended to be the best current assessment.) Using the contents and fluxes associated with each source (including the oceanic content), the $CH_3Br$ lifetime for surface emissions is 1.03 years as before, but for oceanic emissions it is only 0.49 years. An oceanic source puts more $CH_3Br$ in the reservoir with the most rapid destruction. Amazingly, both B3/surface and B3/ocean, with lifetimes differing by a factor of 2, are represented by the same modes and timescales including the long-lived decay modes of 0.91 and 1.83 years, but with different coefficients.

If the {$CH_3Br$, $Br_y$} analysis is extended to longer-lived halogen source gases such as $CH_3CCl_3$, or even those without a tropospheric sink such as $CFCl_3$, the discrepancy between the time scale for ozone recovery and that inferred from the steady state lifetime becomes less. This convergence of the lifetime and the primary mode's time scale happens as the global-mean lifetime (e.g., 50 years for $CFCl_3$) becomes much longer than the slowest transport time scale (e.g., 3-5 years for stratospheric removal). We are now observing the decay of atmospheric $CH_3CCl_3$ following the recent phaseout in production [*Prinn et al.,* 1995; *Montzka et al.,* 1996]. This *e*-folding time is coincidentally expected to be almost identical to the derived steady state lifetime based on surface emissions [*Prinn et al.,* 1995], and we may observe a small residual maximum in the high-latitude lower stratosphere as $CH_3CCl_3$ decays in the atmosphere. For longer-lived gases like $CFCl_3$ the timescale of the primary mode is a few percent less than the lifetime at steady state for surface emissions.

The long-lived, odd-nitrogen source gas $N_2O$, however, is expected to have natural modes and timescales that are significantly shorter than the steady state lifetime because of the photochemical coupling in the {$N_2O$, $NO_y$, $O_3$} system. A preliminary study with this 1-D model that includes coupling of $NO_y$ with $O_3$ depletion and subsequent increased photolysis of $N_2O$ indicates that $N_2O$ perturbations may damp at a rate 10-20% faster than the lifetime.

## Appendix

A 1-D chemical diffusion model of {$CH_3Br$, $Br_y$} for the atmosphere [*Logan et al.*, 1978; *Prather*, 1994] is as follows: mixing ratios solved for at 14 altitudes, z = 0 - 4 - 8 - 12 - 16 - 20 - ... - 52 km; density given by $N = 2.4\times10^{16}$ p $cm^{-3}$ assuming $p = 1000\times10^{-z/16}$ mbar (note that N needs to be scaled by 1.25 for global mean atmospheric mass); diffusion coefficient, $K = 3\times10^5$ $cm^2$ $s^{-1}$ for 0 - 12 km; $K = 3\times10^3$ $cm^2$ $s^{-1}$ at 14 km, increases as 1/p above; chemical loss of $CH_3Br$, $L_1 = 2.166\times10^{-8}$ $s^{-1}$ from 0-10 km ("OH loss" at 1/1.46 per year); $L_1 = 6\times10^{-6}/p^2$ $s^{-1}$ above 10 km (constant above p = 1); chemistry of $Br_y$, every loss of $CH_3Br$ produces $Br_y$; $L_2 = 2.315\times10^{-6}$ $s^{-1}$ from 0-10 km ("rainout" at 1/5 per day); numerics, 2nd-order finite difference, 2nd-order boundary conditions, implicit in time (single-step solution for steady state). The model of {$CH_3Br$} for the ocean [*Lobert et al.*, 1995] is as follows: ocean box (mixed layer) connected to surface atmospheric layer (0-2 km); effective thickness based on solubility and mixed layer depth, $0.5\times10^{24}$ $cm^{-2}$ (versus $4.8\times10^{24}$ $cm^{-2}$ for 0-2 km layer); effective air exchange rate with atmosphere, $3.86\times10^{17}$ $cm^{-2}$ $s^{-1}$; chemical loss of $CH_3Br$, $9.26\times10^{-7}$ $s^{-1}$ (8%/day). Three sample cases are shown (Figure 3): B1, atmosphere alone, 10 ppt $CH_3Br$ @ 0 km, 4.17 ppt $Br_y$ @ 20km (all cases); B2, atmosphere plus ocean, only surface $CH_3Br$ source (ocean at 45% saturation); B3, atmosphere plus ocean, surface and oceanic $CH_3Br$ sources (ocean at 85% saturation).

**Acknowledgments.** This research was supported by NASA's Atmospheric Chemistry Modeling and Analysis Program and NSF's Atmospheric Chemistry Program. I thank R. Cicerone, B. Hannegan, S. Olsen, and anonymous reviewers for helpful comments.

## References

Anbar, A.D., Y.L. Yung, and F.P. Chavez, Methyl bromide: Ocean sources, ocean sinks, and climate sensitivity, *Global Biogeochem. Cycles, 10*, 175-190, 1996.

Bolin, B., and H. Rodhe, A note on the concepts of age distribution and transit time in natural reservoirs, *Tellus, 25*, 58-62, 1973.

Brune, W.H., J.G. Anderson, and K.R. Chan, In situ observations of BrO over Antarctica: ER-2 aircraft results from 54°S to 72°S latitude, *J. Geophys. Res., 94*, 16639-16647, 1989.

Butler, J.H., The potential role of the ocean in regulating atmospheric $CH_3Br$, *Geophys. Res. Lett., 21*, 185-189, 1994.

Carroll, M.A., R.W. Sanders, S. Solomon, and A.L. Schmeltekopf, Visible and near-ultraviolet spectroscopy at McMurdo Station, Antarctica 5: Observations of BrO, *J. Geophys. Res., 94*, 16633-16638, 1989.

Crutzen, P.J., The influence of nitrogen oxides on the atmospheric ozone content, *Q. J. R. Meteorol. Soc., 96*, 320-339, 1970.

Duafala, T., *Methyl Bromide*, Chap. 10, pp. 10.7-8, World Meteorol. Org., Geneva, 1995.

Ehhalt, D.H., The atmospheric cycle of methane, *Tellus, 26*, 58-70, 1974.

Elliott, S., and F.S. Rowland, Nucleophile substitution rates and solubilities for methyl halides in seawater, *Geophys. Res. Lett., 20*, 1043-1046, 1993.

Jackman, C.H., E.L. Fleming, S. Chandra, D.B. Considine, and J.E. Rosenfield, Past, present, and future modeled ozone trends with comparisons to observed trends, *J. Geophys. Res., 101*, 28753-28767. 1996.

Johnston, H.S., Reduction of stratospheric ozone by nitrogen oxide catalysts from supersonic transport exhaust, *Science, 173*, 517-522, 1971.

Lobert, J.M., J.H. Butler, S.A. Montzka, L.S. Geller, R.C. Myers, and J.W. Elkins, A net sink for atmospheric $CH_3Br$ in the east Pacific Ocean, *Science, 267*, 1002-1005, 1995.

Logan, J.A., M.J. Prather, S.C. Wofsy, and M.B. McElroy, Atmospheric chemistry: Response to human influence, *Philos. Trans. R. Soc., London, Ser. A, 290*, 187-234, 1978.

McCulloch, A., Global production and emissions of $CF_2ClBr$ and $CF_3Br$ (halons 1211 and 1301), *Atmos. Environ., Part A, 26*, 1325-1329, 1992.

McElroy, M.B., S.C. Wofsy, and Y.L. Yung, The nitrogen cycle: Perturbations due to man and their impact on atmospheric $N_2O$ and $O_3$, *Philos. Trans. R. Soc. London, Ser. B, 277*, 159-181, 1977.

Molina, M.J., and F.S. Rowland, Stratospheric sink for chlorofluoromethanes: Chlorine atom catalyzed destruction of ozone, *Nature, 249*, 810-814, 1974.

Montreal Protocol on Substances that Deplete the Ozone Layer, final act, Montreal, Que., Canada, Sept. 16, 1987.

Montzka, S.A., J.H. Butler, R.C. Myers, T.M. Thompson, T.H. Swanson, A.D. Clarke, L.T. Lock, and J.W. Elkins, Decline on the tropospheric abundance of halogen from halocarbons: Implications for stratospheric ozone depletion, *Science, 272*, 1318-1322, 1996.

Prather, M.J., Lifetimes and eigenstates in atmospheric chemistry, *Geophys. Res. Lett., 21*, 801-804, 1994.

Prather, M.J., Time scales in atmospheric chemistry: theory, GWPs for $CH_4$ and CO, and runaway growth, *Geophys. Res. Lett., 23*, 2597-2600, 1996.

Prather, M.J., and R.T. Watson, Stratospheric ozone depletion and future levels of atmospheric chlorine and bromine, *Nature, 334*, 729-734, 1990.

Prather, M., P. Midgley, F.S. Rowland, and R. Stolarski, The ozone layer: The road not taken, *Nature, 381*, 551-554, 1996.

Prinn, R., R. Weiss, B. Miller, J. Huang, F. Alyea, D. Cunnold, P. Fraser, D. Hartley, and P. Simmonds, Atmospheric trends and lifetime of trichloroethane and global average OH concentrations based on 1978-1994 ALE/GAGE measurements, *Science, 269*, 187-192, 1995.

Schauffler, S.M., L.E. Heidt, W.H. Pollock, T.M. Gilpin, J.F. Vedder, S. Solomon, R.A. Lueb, and E.L. Atlas, Measurements of halogenated organic compounds near the tropical tropopause, *Geophys. Res. Lett., 20*, 2567-2570, 1993.

Shorter, J.H., C.E. Kolb, P.M.Crill, R.A. Kerwin, R.W. Talbot, M.E. Hines, and R.C. Harriss, Rapid degradation of atmospheric $CH_3Br$ in soils, *Nature, 377*, 717-719, 1995.

Solomon, S., and D.L. Albritton, Time-dependent ozone depletion potentials for short- and long-term forecasts, *Nature, 357*, 33-37, 1992.

Stolarski, R.S., and R.J. Cicerone, Stratospheric chlorine: A possible sink for ozone, *Can. J. Chem. 52*, 1610-1615, 1974.

Toohey, D.W., J.G. Anderson, W.H. Brune, and K.R. Chan, In situ measurements of BrO in the Arctic stratosphere, *Geophys. Res. Lett., 17*, 513-516, 1990.

World Meteorological Organization (WMO), Atmospheric ozone 1985, *Rep. 16*, Global Ozone Res. and Monit. Proj., Geneva. 1986.

WMO, Scientific assessment of ozone depletion: 1991, *Rep. 25*, Global Ozone Res. and Monit. Proj., Geneva, 1992.

WMO, Scientific assessment of ozone depletion: 1994, *Rep. 37*, Global Ozone Res. and Monit. Proj., Geneva, 1995.

Wofsy, S.C., M.B. Mcelroy, and Y.L. Yung, The chemistry of atmospheric bromine, *Geophys. Res. Lett., 2*, 215-218, 1975.

Yvon, S.A., and J.H. Butler, An improved estimate of the oceanic lifetime of atmospheric $CH_3Br$, *Geophys. Res. Lett., 23*, 53-56, 1996.

M. J. Prather, Department of Earth System Science, University of California, Irvine, CA 92697-3100. (e-mail: mprather@uci.edu)

(Received August 13, 1996; revised March 4, 1997; accepted April 2, 1997.)